CrossMark

Fragment-based approaches to TB drugs

CHIARA MARCHETTI, DANIEL S. H. CHAN, ANTHONY G. COYNE* *and* CHRIS ABELL*

Department of Chemistry, University of Cambridge, Lensfield Road, Cambridge CB2 1EW, UK

(*Received 4 August 2016; revised 27 September 2016; accepted 27 September 2016; first published online 2 November 2016*)

SUMMARY

Tuberculosis is an infectious disease associated with significant mortality and morbidity worldwide, particularly in developing countries. The rise of antibiotic resistance in *Mycobacterium tuberculosis* (*Mtb*) urgently demands the development of new drug leads to tackle resistant strains. Fragment-based methods have recently emerged at the forefront of pharmaceutical development as a means to generate more effective lead structures, via the identification of fragment molecules that form weak but high quality interactions with the target biomolecule and subsequent fragment optimization. This review highlights a number of novel inhibitors of *Mtb* targets that have been developed through fragment-based approaches in recent years.

Key words: tuberculosis, fragment-based approaches, medicinal chemistry, cytochrome P450, pantothenate synthetase, EthR, BioA.

INTRODUCTION

Tuberculosis

Tuberculosis (TB) is a disease caused by the pathogen *Mycobacterium tuberculosis* (*Mtb*). According to the World Health Organization (WHO) in 2014 it was estimated that 1·5 million people died as a result of the disease and a further 9·6 million people were infected (WHO Report, 2015). This has been further complicated by the fact that there has been a rise in the multidrug resistant (MDR), extensively drug resistant (XDR) and totally drug resistant (TDR) forms of *Mtb*.

The current drug regimen for the treatment of TB involves a lengthy treatment programme of over 6 months and in some cases this can last 1–2 years in the case of MDR and XDR-TB strains. The drugs used to treat TB have not changed much since the 1960s and there are significant toxic side-effects associated with the long-term usage of these drugs. In recent years, there has been resurgence in interest in TB as a target for drug discovery. The increase in the number of people infected with resistant strains of *Mtb* [e.g. MDR-TB] offers the biggest challenge in tackling this disease and because of this there is the urgent need to develop new drugs against novel targets in *Mtb*. The development and the subsequent FDA approval of the drug Bedaquiline, which targets ATP synthase was a significant step in this respect (Koul *et al*. 2011). This was the first drug to be approved in over 40 years for the treatment of TB.

* Corresponding author: Department of Chemistry, University of Cambridge, Lensfield Road, Cambridge CB2 1EW, UK. E-mail: ca26@cam.ac.uk; agc40@cam.ac.uk

Fragment-based drug discovery (FBDD)

Fragment-based approaches to drug-discovery are now firmly established in both academia and industry. FBDD is now routinely run alongside high-throughput screening (HTS) campaigns and there has been notable successes with certain targets where HTS campaigns have failed. (Congreve *et al*. 2008; Scott *et al*. 2012) In 2016, the second drug developed using this methodology was approved by the FDA following on from Vemurafenib, which was approved in 2011.

The fragment-based approach involves the screening of a fragment library (1000–5000 fragments) against a target using a range of biophysical techniques. The fragments (typically molecular weight <250 Da) bind with affinities of 0·1–5·0 mM, and the biophysical techniques need to have the sensitivity required to detect these interactions. A wide range of biophysical techniques have been explored for fragment screening, including differential scanning fluorimetry, surface plasmon resonance (SPR), ligand- and protein-based Nuclear Magnetic Resonance (NMR) (Mashalidis *et al*. 2013). However, the one technique which has proven crucial for this approach has been X-ray crystallography (Murray and Blundell 2010). This provides a key insight into how fragments bind to the target protein. Once the fragments have been fully characterized the next step is to increase their affinity. The fragment elaboration strategies that are employed include fragment growing, fragment merging and fragment linking. Fragment growing is the strategy used the most frequently and this involves 'growing' a fragment using synthetic organic and medicinal chemistry. Structural information from X-ray crystal structures is a key aspect for fragment growing (Fig. 1).

Parasitology (2018), **145**, 184–195. © Cambridge University Press 2016
doi:10.1017/S0031182016001876

https://doi.org/10.1017/S0031182016001876 Published online by Cambridge University Press

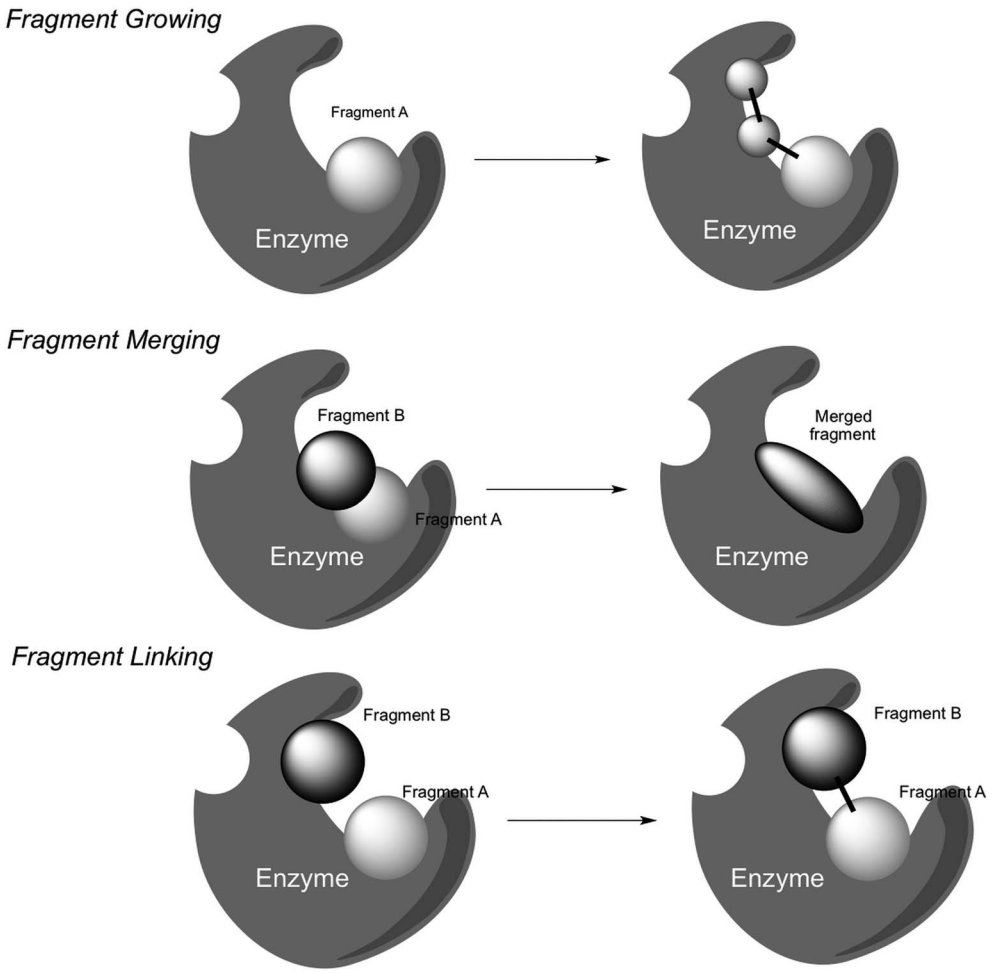


Fig. 1. Fragment elaboration strategies.

Fragment merging is the incorporation of the structural aspects of overlapping fragments, substrates and other ligands. Fragment linking involves the linking of two or more fragments at non-overlapping binding sites. The linking of two fragments is one of the most appealing strategies as the binding affinity of the linked compounds is expected to have a Gibbs free energy greater than the sum of the individual fragment binding energies (superadditivity effect). However, in practice this strategy is one of the most difficult to achieve. These elaboration strategies will be discussed in this review in the context of fragment-based approaches for the development of novel *Mtb* inhibitors.

ENZYME TARGETS FOR TB DRUGS

(a) Coenzyme A (CoA) biosynthetic pathway

The CoA biosynthetic pathway enzymes are validated targets for the treatment of *Mtb* infections. CoA is one of the most widely used of all the enzyme cofactors; it is required by both prokaryotic and eukaryotic cells for fatty acid biosynthesis and breakdown and for respiration, due to its role in the Krebs cycle. The terminal thiol functionality of CoA forms thioesters with carboxylic acids of different lengths (from two carbons group to entire fatty acids) and this specific reactivity allows CoA to act as an acyl group carrier, which is the main role of this cofactor.

The protein members of the CoA biosynthetic pathway have been extensively characterized. The cofactor is the product of two different pathways, the first of which is responsible for the production of panthotenic acid (or vitamin B_5) that is then used as substrate via five enzymatic steps to obtain the final CoA. Because of CoA essentiality, the enzymes involved in the pathway have been proposed as novel targets for the development of drugs for the treatment of *Mtb* infections, with the aim of overcoming the intrinsic resistance to current treatments. In particular, the panthotenic acid pathway fulfils all the requisites required by a broad spectrum antibacterial target: it is essential for mycobacterium survival and is exclusive for bacteria, since eukaryotic cells are not able to produce vitamin B_5 and have to assume it from the extracellular environment (Spry *et al.* 2008).

The panthotenic acid biosynthetic pathway consists of three enzymatic reactions, α-ketoisovalerate

https://doi.org/10.1017/S0031182016001876 Published online by Cambridge University Press

is first transformed into ketopantoic acid by ketopantoate hydroxymethyltransferase (KPHMT product of the panB gene), which is then reduced by ketopantoate reductase (KPR or panE) to pantoic acid. Finally, pantoic acid is condensed with β-alanine [deriving from aspartic acid (Asp) thanks to the activity of aspartate decarboxlase] by panthotenate synthetase (PS or panC) to give pantothenic acid (Webb *et al*. 2002).

The role of PS as a *Mtb* target has been validated in genetic studies by proving that an auxotrophic mutant of *Mtb* defective in panC showed reduced virulence in both immunocompromised and immunocompetent mice (Sambandamurthy *et al*. 2002). Furthermore, the presence of several X-ray crystal structures for the enzyme, in its dimeric apo form as well as in complex with its substrates or the pantoyladenylate intermediate, facilitates the structure-based inhibitor design following the fragment hit identification. This makes PS a very promising target from a FBDD perspective (Wang and Eisenberg 2003).

Ciulli and co-workers explored PS using an integrated biophysical approach [thermal shift, NMR, isothermal titration calorimetry (ITC), X-ray crystallography] for fragment screening and validation (Silvestre *et al*. 2013). A 'rule of three' compliant fragment library of 1250 compounds was screened using thermal shift, with a fixed threshold value (0·5 °C at 10 mM) (Fig. 2). Thirty-nine fragments were identified (3·1% hit rate) and seventeen hits were confirmed to bind using ligand-based NMR techniques (WaterLOGSY and STD). This approach based on the use of several biophysical techniques proves that the success rate obtained by an initial thermal shift screening followed by NMR is higher compared with a NMR-based fragment screen: the same group performed a simplified NMR screen against PS using 52 fragments with the identification of only one ATP-competitive inhibitor, 5-methoxyindole **2** (Hung *et al*. 2009). The fragments were further characterized using ITC where K_D values were measured and were found to be in the range of 0·5 to 1·7 mM. Subsequent examination of the binding of the fragments to PS with X-ray crystallography allowed the identification of three different binding pockets in the PS active site: the recognition site of the ATP adenine motif, the pantoate-binding site (P1) and the pyrophosphate and β-alanine-binding pocket (P2).

This initial work was followed by fragment elaboration strategies using structure-based approaches. 5-Methoxyindole **2**, K_D of 1·1 mM (LE = 0·36), was found to bind at the recognition site of the ATP adenine motif in the crystal structure and was selected as a startpoint for a fragment growing approach aimed at exploring the P1 and P2 pockets (Hung *et al*. 2009). The introduction of a carboxylate group at either the C-2 or N-1 position halved the K_D value (0·5 mM) while maintaining a high LE (~0·30). The carboxylic acid group at C-2 was replaced by an acyl sulfonamide, a flexible moiety that maintains the acidity of the carboxylic acid and allows the compound to bend in either P1 or P2 pockets. Among different acyl sulfonamides, **3** carrying a methylpyridine group able to occupy P2, was found by ITC to give a K_D of 29 μM (LE = 0·26). The introduction of the acetate on N1 (**4**) gave an increase in the affinity (K_D) to 1·5 μM.

Benzofuran-2-carboxylic acid **1** was found to bind in P1 simultaneously with **2**, 3·1 Å away from the binding site of the methoxyindole. Structural data were used to guide the development of an acylsulfonamide linker to merge the two fragments into a single lead molecule, **7** (K_D = 1·8 μM, LE = 0·26). The X-ray crystal structure of compound **7** revealed that the linked compound maintains the binding modes of the original fragments. In a further study, compounds **3** and **7** were explored from a group efficiency (GE) analysis in an effort to improve their binding affinities, (Hung *et al*. 2016). GE analysis showed that the components that had the highest positive impact to the binding were the indole group (GE = 0·75) and the alkyl carboxylate substituent on N1 (GE between 0·35 and 0·43). The synthesis of several acyl sulphonamides analogues led to a series of inhibitors, the best compound **5** having a K_D of 0·20 μM (LE = 0·30) and an IC_{50} of 5·7 μM. Based on the X-ray crystallographic data, a methylene linker was introduced between the sulfonamide and the phenyl group in order to push the trifluoromethyl group deeper into the pantoate-binding site, giving compound **6** with an IC_{50} value of 250 nM.

(b) Cytochrome P450 (CYP121)

The cytochrome P450 enzymes (CYPs) are potential targets for the treatment of *Mtb* infections. The discovery of the unusually large number of CYPs encoded in the mycobacterium genome (20 in the 4·4 Mb *Mtb* H37Rv genome *vs* 57 in the 3 Gb human genome) underlines the importance of this class of enzymes, mainly in relation to the virulence and the survival of the mycobacterium (Cole *et al*. 1998; Hudson *et al*. 2012*a*, *b*). This family of mono-oxygenase enzymes catalyses the oxidation of organic substrates due to the presence of a heme cofactor. The unique cytosolic localization of bacterial CYPs as well as their use of a different electron donor system, more specifically a two-component system comprising of a FAD-containing ferredoxin reductase and an iron-sulphur cluster containing ferredoxin, represent good starting points for the development of selective inhibitors.

The structures and specific functions of only five *Mtb* CYPs have been disclosed so far, CYP51B1 is

https://doi.org/10.1017/S0031182016001876 Published online by Cambridge University Press

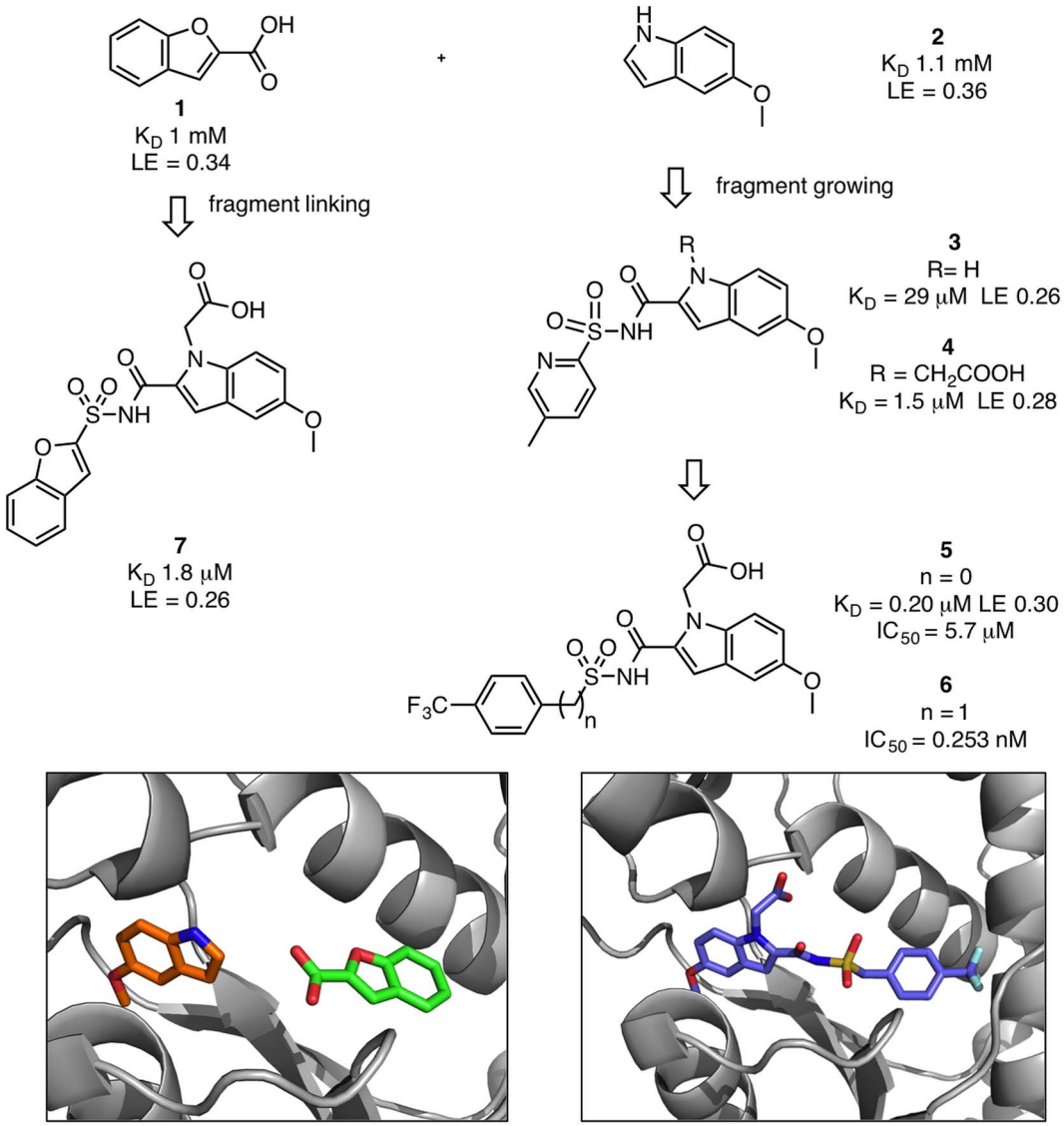


Fig. 2. Fragment growing and merging strategies leading to the development of inhibitors of pantothenate synthetase (PS) (PDB codes: 3IMG, 4MUK).

involved in the biosynthesis of sterols, while CYP124, CYP125 and CYP142 constitute a pathway for the metabolism of host-derived steroids. CYP121 is the most promising TB drug target among the different CYPs; it is exclusive to *Mtb* and mediates the formation of mycocyclosin catalysing the formation of a C–C bond between the two tyrosine residues of the substrate cyclodityrosine (cYY), the product of the cyclodipeptide synthetase *Rv2275* that is associated in an operon-like structure with *Rv2276*, the gene encoding for CYP121 (Belin *et al*. 2009). This unusual reaction catalysed by CYP121 takes place in a unique binding site, thus improving the chance of achieving selectivity over other CYPs. Further evidence for CYP121 essentiality was shown that it was impossible to obtain a CYP121 knock out mutant unless a complementary vector is present (McLean *et al*. 2008). The *apo* X-ray crystal structure of CYP121 was solved to high resolution revealing a highly constrained active site and allowing the protein to be considered a strong candidate as potential target from a FBDD point of view (Leys *et al*. 2003). While a number of azole antifungals are known to inhibit CYP121 via a type II azole-heme coordination, they possess limited selectivity over other mammalian CYPs.

Hudson and co-workers explored a fragment-based approach to targeting CYP121 (Hudson *et al*. 2012*b*) (Fig. 3). A fragment screen was conducted using an fluorescence-based thermal shift analysis as a first-line screen on a library of 665 'rule of three' compliant fragments, which identified 66 hits causing an increase of the melting temperature of CYP121 by + 0·8 °C or greater at a concentration of 5 mM (hit rate of 9·9%), 46% of these hits were confirmed using NMR (STD and WaterLOGSY) which also showed cYY displacement, suggesting a potential binding mode into the

https://doi.org/10.1017/S0031182016001876 Published online by Cambridge University Press

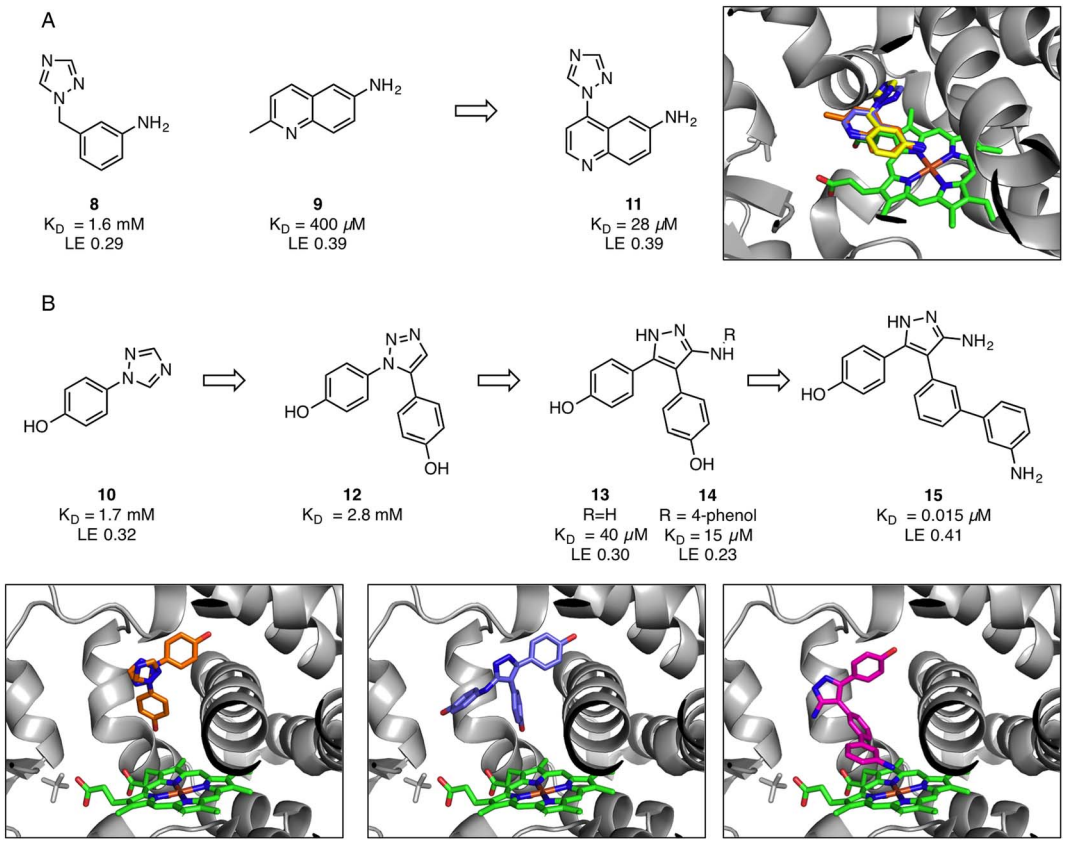


Fig. 3. (a) Fragment merging strategies targeting CYP121 (PDB codes: 4G45, 4G44, 4G1X) (b) Fragment elaboration strategies targeting CYP121 (PDB codes: 4G47, 4KTL, 5IBE).

active site of the protein. These fragments were soaked into CYP121 crystals and four X-ray crystal structures were obtained, all with the fragments located in the CYP121 active site. Two main distinct binding modes were observed: fragments **8** and **9** were characterized by a type II heme-binding mode via the arylamine nitrogen and π–π interactions with the prosthetic group, while fragment **10** (characterized by the ability to bind in two different conformations) adopted an unusual binding mode with the azole moiety not involved in the coordination of the iron. The binding affinity of the fragments was determined by ITC, with the best hit being **9** ($K_D = 400\,\mu M$, LE = 0·39). Fragment merging strategies were applied to the two overlapping heterocycles and resulted in a small library of aminoquinolines with improved affinity compared with the initial hits, the best derivative was 1,2,4-triazolylquinoline **11** with a K_D of 28 μM (LE = 0·39). The analysis of the analogues of **11** showed that the aniline group was the main contributor to the binding (GE = 2·6 kcal mol^{-1}). The crystal structure of **11** in complex with CYP121 proved that the compound retains the binding mode of the parent fragments, with the arylamine involved in heme coordination and the five membered ring interacting via a water-mediated H bond with a heme carboxylate.

Additional merging strategies with the fragments binding further from the heme did not improve the binding affinities. In particular, compound **12**, derived from two different configurations of fragment **10**, proved to be less active than the original fragment hit ($K_D = 2{\cdot}8$ mM), with quantum mechanical calculations suggesting this result was due to a steric clash of the *ortho*-hydrogen atoms of the opposite phenol groups (Hudson *et al*. 2013). The replacement of the original five-membered 1,2,4-triazole ring with an aminopyrazole led to **13**, with a K_D of 40 μM which was a 70-fold more potent than the original fragment **12**. The growth into the large CYP121 water-filled active site finally yielded **14**, whose additional phenol ring protrudes into the active site creating H-bonds with the interstitial solvent. The compound was the first high affinity ligand for CYP121 ($K_D = 15\,\mu M$, LE = 0·23) whose binding was not due to heme coordination. This compound was the subject of further medicinal chemistry efforts aimed at improving the potency and addressing the low ligand efficiency of the compound (Kavanagh *et al*. 2016). A deconstruction approach, pursued by the synthesis of retro-fragments of the derivative, defined the GE for the tree aromatics ring, from which it emerged that the aromatic ring linked to the nitrogen was responsible for a small contribution (GE between −0·03 and 0·08),

https://doi.org/10.1017/S0031182016001876 Published online by Cambridge University Press

therefore it was removed. Examination of the binding mode showed a possible vector of growth from the meta-position of the aromatic ring closer to the aniline group towards the heme cofactor, as a way to incorporate a metal binding group. The introduction of a 3-aminophenyl group gave **15**, which exhibited excellent affinity for CYP121 with a $K_D = 0{\cdot}015\ \mu M$ (LE = 0·41) which to date is the highest affinity compound developed for CYP121.

(c) Protein tyrosine phosphatase (PTP)

The reversible phosphorylation of tyrosine in both prokaryotic and eukaryotic cells is at the heart of a large number of biological processes, where it acts as key regulator in the protein functionality of all living systems. This process is mediated by the opposite action of tyrosine phosphorylases and phosphatases (Tonks, 2006). In prokaryotic cells, PTPs are implicated in virulence and mediate the modification of host proteins in order to favour the spread of the microorganism. From the analysis of the *Mtb* genome, the presence of two PTPs, MPtpA and MPtptB, has been revealed (Cole *et al*. 1998). The lack of endogenous tyrosine phosphorylation in *Mtb* suggests that *Mtb* PTPs act as modulators of the macrophage proteins leading to attenuation of the host immune defences by interfering with the interferon-γ signalling pathway. Although not essential for extracellular survival of *Mtb in vitro*, the target has been validated by proving that genetic depletion of MPtpB impairs the ability of the pathogen to survive in the presence of interferon-γ activated macrophages in a guinea pig model, leading to a 70-fold lower bacillary load compared with the parental strain (Singh *et al*. 2003). Further, the peculiar localization outside the highly impermeable mycobacterium cell wall improves the appeal of *Mtb* PTPs as drug targets. The issues arising from the highly conserved amino acidic sequence of the PTP active site within different species have been overcome with the discovery of unique secondary binding sites that share less homology and permit the achievement of selectivity (Barr *et al*. 2009). There have been a number of efforts to target these enzymes and selective inhibitors have been obtained by using a Click chemistry approach to create bidentate ligands targeting the main active site and the secondary site at the same time, as well as from HTS of natural compound libraries (Tan *et al*. 2009; Schmidt *et al*. 2011; Mascarello *et al*. 2013).

Ellman and co-workers employed a new substrate-based fragment approach termed 'substrate activity screening' (SAS) to identify new MPtpB inhibitors. In this approach, the fragment hits were identified from a library of PTPs potential substrates (a set of 140 structurally diverse, low molecular weight *O*-aryl phosphates with different structural features) and subsequently underwent a fragment elaboration and optimization process. Finally the phosphate group of the optimized substrates was replaced by a phosphate isostere, thus converting an optimal substrate into a selective and potent inhibitor (Soellner *et al*. 2007) (Fig. 4A).

The initial screening yielded seven promising scaffolds acting as MPtpB substrates (K_M between 267 and 24 μM) (Fig. 4A). Among the hits, the biphenyl derivative **16** with a K_M of 86 μM was selected for further medicinal chemistry efforts because of the favourable drug-like properties of the biphenyl scaffold, which is recognized as a privileged structure. The introduction of a *m*-trifluoromethyl and *p*-fluoro substituents on the original scaffold allowed a 4- and 2-fold decrease in K_M, respectively, while merging both the substitution patterns provided **17** ($K_M = 13\ \mu M$). Compound **17** was converted from substrate to inhibitor via replacement of the phosphate group with the monoacidic isosteres, isothiazolidinone and isoxazole carboxylic acid. The latter furnished a promising inhibitor **18** with K_i of 2·50 μM ($K_i = 8{\cdot}80\ \mu M$ for the isothiazolidinone). In order to further improve the potency of the compound, modifications inspired by the structural similarity between the fragment hits previously identified were applied, generating isoxazole **19,** which is currently the most potent inhibitor of MPtpB reported to date with a K_i of 0·22 μM and >200-fold selectivity over the MPtpA and different human PTPs.

Ellman and co-workers have also conducted a SAS screening on MPtpA by creating a small library of difluoromethylphosphonic acids (Rawls *et al*. 2009) (Fig. 4B). The most promising compound obtained from the preliminary SAR investigations was the benzanilide **20** ($K_{ib} = 24\ \mu M$). Different substituents were then introduced on the phenyl ring mounted on the nitrogen of the amide functionality; introduction of electron withdrawing group, especially in the meta- or para-position gave excellent affinity. Compound **21** was the best derivative identified ($K_i = 1{\cdot}4\ \mu M$), with >70-fold selectivity over MPtpB thus allowing the compound to be considered a good molecular probe for the investigation of the different biological roles of the two enzymes. Further elaboration aimed at replacing the amide group yielded **22** as the best derivative ($K_i = 3{\cdot}1\ \mu M$), showing the difficulty of replacing the amide.

(d) 7,8-Diaminopelargonic acid (DAPA) synthase (BioA)

The biotin biosynthetic pathway in *Mtb* has emerged as a potential drug target because of its essentiality for *Mtb* survival both *in vitro* and *in vivo*, whereas this pathway does not exist in human hosts. 7,8-Diaminopelargonic acid (DAPA) synthase (BioA), which catalyses the second step of

https://doi.org/10.1017/S0031182016001876 Published online by Cambridge University Press

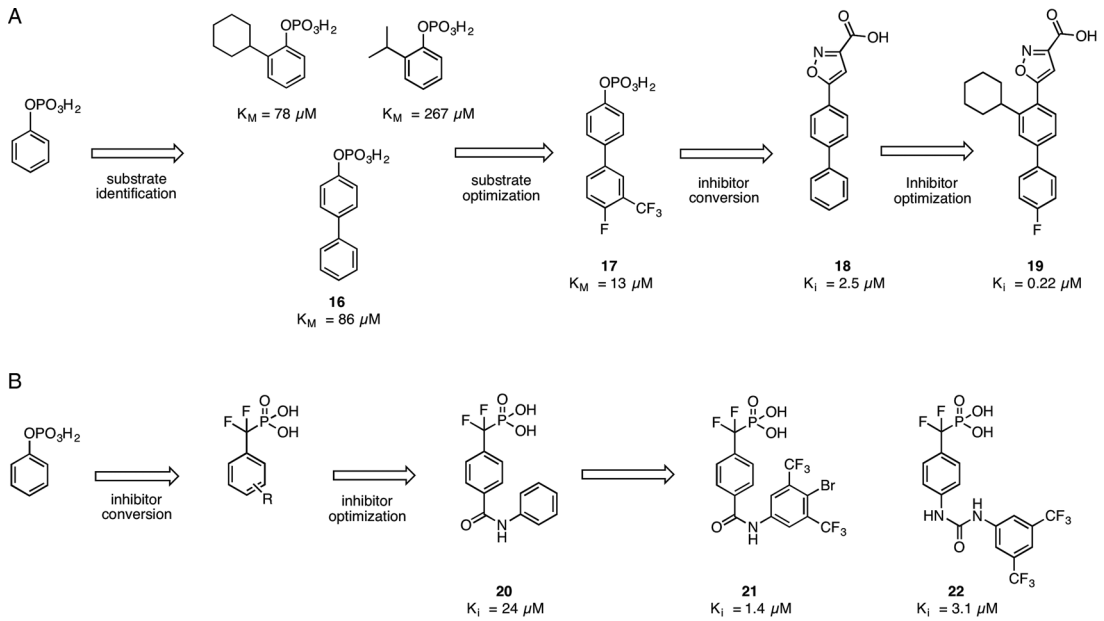


Fig. 4. Substrate activity screening targeting (A) MPtpB and (B) MPtpA.

biotin biosynthesis from pimeloyl-CoA, was shown to be important for persistence in a murine model of TB. (Park *et al*. 2011) Furthermore, biotin deprivation of the Δ*bioA Mtb* mutant led unusually to cell death, rather than growth arrest, indicating the possibility of targeting BioA as an anti-tubercular strategy. Previous efforts had identified the microbial natural product amiclenomycin (ACM) and its derivatives as inhibitors of *Mtb* BioA in bacterial cells, but these showed low efficacy in animal models, while other ACM analogues showed improved stability but lower potency. (Hotta *et al*. 1975; Shi and Aldrich 2012; Woong Park *et al*. (2011)).

Finzel and co-workers were the first to apply FBDD to identify new inhibitors of BioA (Dai *et al*. 2014). A library of *ca*. 1000 fragments was screened at 5 mM using a thermal shift assay. Nine compounds exhibited positive T_m shifts larger than 2 °C, while 12 molecules showed negative shifts greater than 2 °C. In particular, 2-(aminomethyl)-benzothiazole **23** (Fig. 5) showed a negative shift of −7·0 °C at 5 mM, and was subjected to crystallization with BioA. The results showed that compound **23** bound to a pocket adjacent to the oxidized pyridoxamine (PLP) co-factor, forming hydrogen-bonding interactions with both PLP and several residues of the enzyme, mimicking interactions made by the natural substrate 7-keto-8-aminopelargonic acid (KAPA). The binding of **23** to BioA was further confirmed by ligand-based STD NMR experiments.

In the structure-guided fragment optimization campaign, nine commercially available benzothiazoles related to **23** were evaluated using the thermal shift assay. Of these analogues, the hydrazine derivative **24** exhibited the largest negative thermal shift of −19 °C. Interestingly, addition of **24** to either PLP-bound or apo-BioA led to the formation of a deep red colour. The crystal structure of **24** with BioA showed the hydrazine group formed a covalent adduct with the PLP aldehyde to form a *cis*-azo quinonoid moiety. Additionally, and unlike compound **23**, the molecule also induced significant and diverse conformational shifts in multiple regions of the enzyme, which was determined using X-ray crystallography. Kinetic experiments showed that **24** was a competitive reversible inhibitor of BioA with respect to the amino donor S-adenosyl methionine (SAM) ($K_i = 10{\cdot}4 \pm 0{\cdot}6\ \mu M$) and uncompetitive with respect to KAPA ($K_{iu} = 85{\cdot}4 \pm 3{\cdot}4\ \mu M$). The authors proposed that by forming a reversible covalent adduct between **24** and the PLP cofactor, subsequent reaction of PLP-BioA with SAM is prevented. Interestingly, while isoniazid also bound covalently to PLP in a co-crystal structure with BioA, it showed no inhibition in the BioA activity assay, suggesting that the isoniazid-PLP adducts observed crystallographically are very easily dissociated upon exposure to the natural substrates.

The unexpected conformational shifts of BioA induced by these molecules could potentially provide fertile grounds for the development of inhibitors that stabilize catalytically-inactive forms of the enzyme. This study also highlights that the destabilizing fragment hits, i.e. those that induce a negative thermal shift, can also provide worthwhile scaffolds for investigation, which stands in contrast to most fragment screening campaigns where only molecules inducing positive thermal shifts are considered.

(e) Protein antigen 85C

An interesting approach was employed by Schade and co-workers in the development of inhibitors

https://doi.org/10.1017/S0031182016001876 Published online by Cambridge University Press

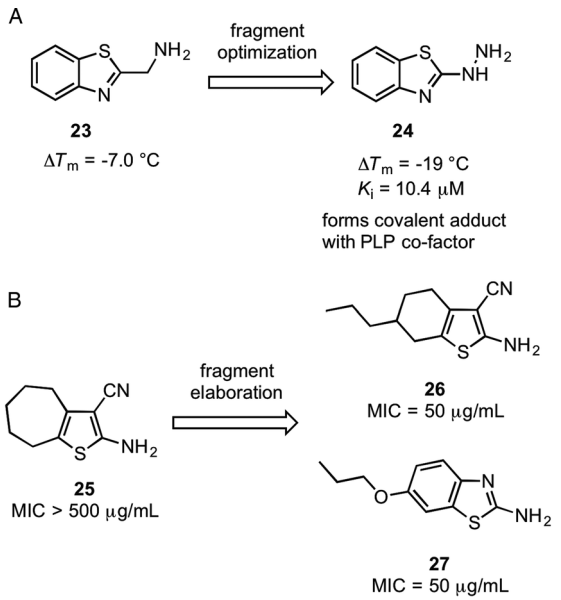


Fig. 5. (A) Fragment optimization of a BioA inhibitor. (B) Fragment-based discovery of Ag85C inhibitors.

targeting *Mtb* antigen 85C (Ag85C) (Scheich *et al*. 2010). Mycolyl transferases antigens (Ag) 85A, 85B and 85C catalyse the transfer of mycolates between trehalose monomycolate and trehalose mycolate (TDM), which are important components of the mycolyl–arabinogalactan–peptidoglycan (mAGP) complex of the mycobacterial cell wall (Belisle *et al*. 1997). Genetic knockout of Ag85A abolished *Mtb* replication in human and mouse macrophages, while knockout of the Ag85C gene significantly lowered the amount of mycolic acids linked to the cell wall (Jackson *et al*. 1999). Thus, inhibition of the Ag85A-C enzymes represents a potential strategy to inhibit the growth of *Mtb*.

Wary of the poorly drug-permeable nature of the mycobacterial cell wall, the top six hits identified by protein-observed ^{15}N-HSQC NMR spectroscopy from a library of 5000 synthetic fragments were immediately subjected to whole-cell assays before further optimization of the compounds. Only one of six compounds, **25** (Fig. 5), showed growth inhibitory activity against *M. smegmatis*, a model strain that shares Ag85A and Ag85C with *Mtb*, but not against *Escherichia coli* and *Bacillus subtilis*, which lack the Ag85 gene family. While an X-ray co-crystal structure could not be obtained, ^{15}N-HSQC NMR analysis indicated that **25** binds to the active site or directly adjacent site of Ag85C. Derivatization of **25** afforded molecules **26** and **27** as the top analogues that inhibited the growth of both *Mtb* H37 and MDR *Mtb*. Comparison of the structures of **26** and **27** with the known substrates and inhibitors suggested that the alkyl chain of the molecules binds to the mycolyl channel of Ag85C, while the heterocyclic moiety binds to the trehalose recognition site. Notably, this study was the first to establish Ag85C as a therapeutic target for MDR *Mtb*. Additionally, this study highlights the possibility that whole-cell assays can be used very early on in the fragment optimization process.

(f) EthR

Ethionamide is a second-line drug used for treating multidrug-resistant *Mtb*. Mechanistically, it functions as a prodrug that is activated by EthA, a flavin-containing monooxygenase enzyme in *Mtb* EthA (Vannelli *et al*. 2002). EthA catalyses the formation of an ethionamide-NAD adduct that inhibits the 2-*trans*-enoyl reductase enzyme InhA, thereby leading to the impairment of the type II fatty acid synthase system (FAS II) in *Mtb*. However, the efficacy of ethionamide is reduced by the activity of EthR, a TetR-type transcriptional repressor that reduces the expression of EthA (Engohang-Ndong *et al*. 2004). Therefore, the inhibition of EthR would be expected to enhance the expression of EthA, thus potentiating the efficacy of ethionamide and allowing for reduced dosages of the drug to be used.

EthR exists as a homodimer in solution, and each monomer is comprised nine α-helices. The first three α-helices of each monomer comprise the DNA-binding 'head', and the two heads of the dimer must be in close proximity in order for EthR to bind to DNA. However, in the crystal structures of EthR with adventitious hexyl octanoate or 1,4-dioxane molecules, the DNA-binding heads are shifted apart by some 18 Å, resulting in a conformation that is incompatiable for binding to DNA (Dover *et al*. 2004; Frénois *et al*. 2004). Previous studies by the groups of Baulard and Deprez found that molecules capable of inhibiting the DNA-binding of EthR could boost ethionamide activation both *in vitro* and *in vivo*, validating EthR as a potential *Mtb* target (Willand *et al*. 2009; Flipo *et al*. 2011; Flipo *et al*. 2012*a*, *b*).

In 2014, the groups of Willand and Deprez applied different fragment-based methods to discover novel inhibitors of EthR (Villemagne *et al*. 2014). The starting fragment **28** (Fig. 6) was observed in an X-ray co-crystal structure to bind twice to each EthR monomer; once in the D1 'known binding pocket', and once in the region defined by the subpockets D2 and D2′. Fragment **28** showed very weak stabilization of EthR in a thermal shift assay ($\Delta T_m = +0{\cdot}1$ °C), but was inactive against *Mtb* growth in macrophages ($EC_{50} > 10\ \mu M$). Adopting a fragment growing approach, a virtual library of 976 derivatives of **28** was designed and docked against the crystal structure of EthR *in silico* in order to identify analogues that could grow out of the relatively thin and linear D1 pocket. Ten high-scoring molecules from the virtual screening campaign were synthesized and tested *in vitro*,

https://doi.org/10.1017/S0031182016001876 Published online by Cambridge University Press

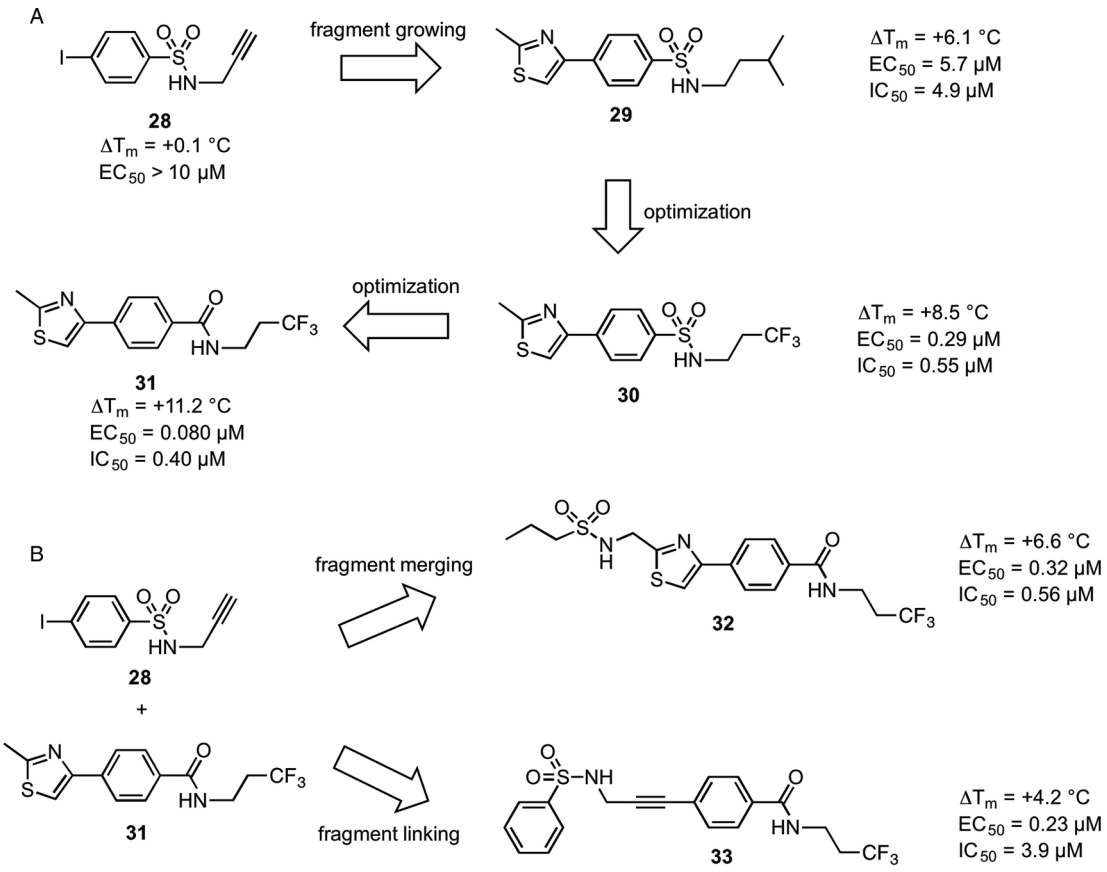


Fig. 6. Fragment strategies to develop inhibitors of EthR. (A) Fragment growing, (B) fragment merging and fragment linking.

from which the 2-methylthiazol-4-yl derivative **29** (ΔT_m = + 6·1 °C, EC_{50} = 5·7 μM), emerged as the top candidate. Four analogues of **29** bearing various modifications to the isopentyl tail of the sulfonamide group were designed and synthesized. The trifluoropropyl-substituted compound **30** (ΔT_m = + 8·5 °C, EC_{50} = 0·29 μM) showed 20-fold higher *in vitro* potency than lead **29**, and was also more effective against EthR DNA-binding as measured using an SPR assay (IC_{50} = 0·55 μM *vs* 4·9 μM for **29**). Replacing the sulfonamide linker with an amide moiety generated compound **31**, the most potent compound of this series (ΔT_m = +11·2 °C, EC_{50} = 0·08 μM, IC_{50} = 0·4 μM). An X-ray crystal structure of **31** with EthR showed that the molecule was successfully grown out of the D1 pocket into the D2 pocket, and additionally, revealed that **31** not only recapitulated the important H-bonding interaction with Asn179 as observed for the original fragment **28**, but also formed a new H-bond with Asn176, which could account for its improved activity over lead structures **29** and **30**, which lack this second interaction.

Two molecules of the starting fragment **28** could be accommodated within the binding channel of an EthR monomer. Fragment merging and fragment linking approaches were also attempted using the optimized compound **31** and a second molecule of fragment **28**; this generated the merged compound **32** and the linked compound **33**, respectively. However, these two molecules showed reduced potency compared to compound **31**, possibly due to lowered solubility as the number of heavy atoms increased, as well as limitations in the choice of connecting groups when linking or merging the two scaffolds together while maintaining the desired interactions. Thus, the authors concluded that the fragment growing strategy was more suitable for exploring the chemical space of the relatively rigid and lipophilic EthR ligand-binding pocket.

In 2014, a fragment-based strategy to target EthR was reported by Surade *et al*. (2014). A library of 1250 fragments were screened against EthR using a thermal shift assay, and 86 fragments were identified which gave ΔT_m values greater than +1·0 °C. These were subsequently tested in an SPR assay to measure their ability to inhibit the EthR–DNA interaction. Of these 86 fragments, 45 fragments inhibited the EthR–DNA interaction by more than 10% at 500 μM, giving a final hit rate of 3·6%. A number of fragments were successfully crystallized with EthR. Of interest was an amide **34** (IC_{50} = 280 μM), which bound twice to a single EthR monomer, together with two molecules of 1,4-dioxane. Interestingly, the binding of this compound appeared to induce significant conformational changes in the structure

https://doi.org/10.1017/S0031182016001876 Published online by Cambridge University Press

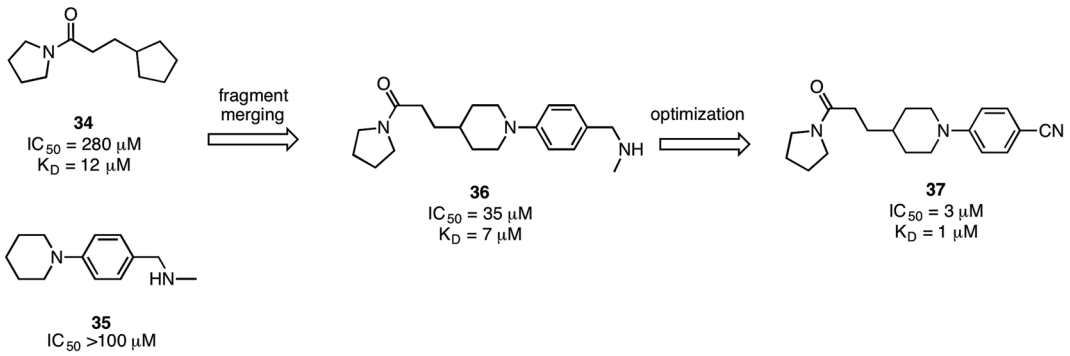


Fig. 7. Fragment merging strategies to develop inhibitors of EthR.

of the protein, particularly movements in the side chains of Phe184 and Glu125, which allowed the second molecule to occupy a previously unexploited cavity in EthR. As two molecules effectively spanned the entire binding channel, a fragment linking strategy was pursued. Dimeric molecules with different linker regions were docked against EthR *in silico* using GOLD, and the results showed that disulphide and amide linkers offered suitable geometry for the fragments to retain their original binding conformation. Five linked molecules were synthesized, and the most potent compound against EthR–DNA-binding activity ($IC_{50} = 0{\cdot}97\ \mu M$) was linked using a disulphide group. Among the dimeric molecules, the disulphide-linked compounds showed significantly higher potency than the amide-linked compounds, which was attributed to the rigidity of the amide bond preventing individual arms of the molecule from forming favourable hydrophobic or hydrogen bond interactions with the binding site. A crystal structure of the linked compounds with EthR showed that the molecule maintained the same overall binding mode as with the starting fragment, including the key hydrogen-bonding interaction with Asn179.

Following on from this work, Abell and co-workers have employed a fragment merging strategy to generate improved inhibitors of EthR (Nikiforov *et al*. 2016). In X-ray crystal structures, fragments **34** and **35** each bound twice to the EthR monomer, and together the two fragments spanned the entire length of the EthR-binding cavity. Merging of fragments **34** and **35** yielded lead structure **36** ($IC_{50} = 35\ \mu M$), which showed an 8-fold improvement in the inhibition of EthR–DNA-binding activity compared with fragment **34** ($IC_{50} = 280\ \mu M$). X-ray crystal analysis revealed that **36** recapitulated the binding poses of the two initial fragments, including the key hydrogen bonding interaction with Asn179, justifying the use of the fragment merging strategy. Structural exploration around the lead compound **36** by SAR generated nitrile **37**, which showed a 5-fold increase in binding affinity as measured by ITC ($K_D = 1\ \mu M$) and a 10-fold improvement in EthR-DNA-binding inhibition ($IC_{50} = 3\ \mu M$). Interestingly, replacement of the amide group of **37** with a urea functionality and/or substitution of the nitrile group with an ester gave molecules with comparable potency, suggesting that these compounds could represent a privileged scaffold for EthR binding. An attempt to merge together one molecule of **34** and two molecules of **35** was comparatively less successful, as the molecules generated, although exhibiting high thermal shift values (+8·3–9·2 °C against EthR) showed reduced ability to perturb the EthR–DNA interaction compared with **36**. However, none of the merged molecules in this study were able to boost ethionamide activity in infected macrophages, which the authors attributed to their inability to penetrate the mycobacterial envelope and/or the host cell membrane (Fig. 7).

While the literature contains successful examples of inhibitors developed from fragment-based approaches there still remains a number of shortcomings to this technique. Phenotypic or HTS identifies compounds that are cell permeable early on in the drug discovery process. However, fragment-based approaches use the isolated enzyme of interest and consequently the elaborated compounds are not screened for cell permeability until much later. Optimizing cell permeability at the later stages of development can prove challenging. One key aspect of the fragment-based approach is that the target protein needs to be isolated in a stable form and in sufficient quantities for screening. The target also needs to be crystallizable for X-ray protein crystallography in order to determine the binding mode of the fragments. These factors affect what targets can be screened. Without a stable, high yielding expression of the target the fragment-based approach is difficult.

Fragment libraries are normally composed of flat heterocycles and these tend to lead to compounds with these heterocycles at their core. Antibacterial drugs which are typically derived from natural products can have multiple chiral centres and oxygen-containing functional groups. Such scaffolds are underrepresented in fragment libraries, and it could be difficult to develop compounds using this approach against these targets using the fragment

https://doi.org/10.1017/S0031182016001876 Published online by Cambridge University Press

based approach. There have been efforts to include more '3D like' fragments in screening libraries; however, the success of these has been somewhat limited.

Within our own laboratory we have had a number of successes with a range of targets using fragment-based approaches ranging from protein–protein, protein–ligand and protein–DNA interactions. However, in some cases this approach has proved unsuccessful and in the case of shikimate kinase, an anti-tubercular target, we were unable to get any validated fragment hits (K. Bromfield, D. Osborne, S. Surade, T.L. Blundell, C. Abell, unpublished observation). We have also had a long-standing interest in the cytochrome P450s from *Mtb* and while CYP121 (see above) was successfully targeted using this approach, other cytochrome P450s such as CYP144 have proved much more difficult to identify fragment hits (M.E. Kavanagh, C. Abell unpublished observation). Each target needs to be taken on its own individual merits and it is not a case that what works for one target will necessarily work for another. However, on the flip side fragment-based approaches have been shown to be successful with challenging targets such as GPCR's and protein–protein interactions where traditional HTS has failed.

Concluding remarks

Fragment-based approaches to drug discovery have been utilized on several TB drug discovery projects in both academia and industry. This has enabled the development of potent inhibitors of a range of targets. With the emergence of drug resistant strains of *Mtb* this new approach to the design of possible therapeutics is a welcome addition to our armoury.

FINANCIAL SUPPORT

C. M. was supported by the Bill and Melinda Gates Foundation (Hit-TB). D. S. H. C. was supported by a Croucher Cambridge International Scholarship awarded in conjunction between the Croucher Foundation and the Cambridge Overseas Trust.

REFERENCES

Barr, A. J., Ugochukwu, E., Lee, W. H., King, O. N., Filippakopoulos, P., Alfano, I., Savitsky, P., Burgess-Brown, N. A., Müller, S. and Knapp, S. (2009). Large-scale structural analysis of the classical human protein tyrosine phosphatome. *Cell* **136**, 352–363.

Belin, P., Le Du, M. H., Fielding, A., Lequin, O., Jacquet, M., Charbonnier, J. B. Lecoq, A., Thai, R., Courçon, M., Masson, C., Dugave, C., Genet, R., Pernodet, J. L. and Gondry, M. (2009). Identification and structural basis of the reaction catalyzed by CYP121, an essential cytochrome P450 in *Mycobacterium tuberculosis*. *Proceedings of the National Academy of Sciences of the United States of America* **106** (18), 7426–7431.

Belisle, J. T., Vissa, V. D., Sievert, T., Takayama, K., Brennan, P. J. and Besra, G. S. (1997). Role of the major antigen of *Mycobacterium tuberculosis* in cell wall biogenesis. *Science* **276**, 1420–1422.

Cole, S. T., Brosch, R., Parkhill, J., Garnier, T., Churcher, C., Harris, D., Gordon, S. V., Eiglmeier, K., Gas, S., Barry, C. E., Tekaia, F., Badcock, K., Basham, D., Brown, D., Chillingworth, T., Connor, R., Davies, R., Devlin, K., Feltwell, T., Gentles, S., Hamlin, N., Holroyd, S., Hornsby, T., Jagels, K., Krogh, A., McLean, J., Moule, S., Murphy, L., Oliver, K., Osborne, J. *et al.* (1998). Deciphering the biology of *Mycobacterium tuberculosis* from the complete genome sequence. *Nature* **393**, 537–544.

Congreve, M., Chessari, G., Tisi, D. and Woodhead, A. J. (2008). Recent developments in fragment based drug discovery. *Journal of Medicinal Chemistry* **51**, 3661–3680.

Dai, R., Wilson, D. J., Geders, T. W., Aldrich, C. C. and Finzel, B. C. (2014). Inhibition of *Mycobacterium tuberculosis* transaminase BioA by Aryl Hydrazines and Hydrazides. *ChemBioChem* **15**, 575–586.

Dover, L. G., Corsino, P. E., Daniels, I. R., Cocklin, I. R., Tatituri, V., Besra, G. S. and Fütterer, K. (2004). Crystal Structure of the TetR/CamR Family Repressor *Mycobacterium tuberculosis* EthR Implicated in Ethionamide Resistance. *Journal of Molecular Biology* **340**, 1095–1105.

Engohang-Ndong, J., Baillat, D., Aumercier, M., Bellefontaine, F., Besra, G. S., Locht, C. and Baulard, A. R. (2004). EthR, a repressor of the TetR/CamR family implicated in ethionamide resistance in mycobacteria, octamerizes cooperatively on its operator. *Molecular Microbiology* **51**, 175–188.

Flipo, M., Desroses, M., Lecat-Guillet, N., Dirié, B., Carette, X., Leroux, F., Piveteau, C., Demirkaya, F., Lens, Z., Rucktooa, P., Villeret, V., Christophe, T., Jeon, H. K., Locht, C., Brodin, P., Déprez, B., Baulard, A. R. and Willand, N. (2011). Ethionamide boosters: synthesis, biological activity, and structure–activity relationships of a series of 1,2,4-Oxadiazole EthR inhibitors. *Journal of Medicinal Chemistry* **54**, 2994–3010.

Flipo, M., Desroses, M., Lecat-Guillet, N., Villemagne, B., Blondiaux, N., Leroux, F., Piveteau, C., Mathys, V., Flament, M. P., Siepmann, J., Villeret, V., Wohlkönig, A., Wintjens, R., Soror, S. H., Christophe, T., Jeon, H. K., Locht, C., Brodin, P., Déprez, B., Baulard, A. R. and Willand, N. (2012*a*). Ethionamide boosters. 2. combining bioisosteric replacement and structure-based drug design to solve pharmacokinetic issues in a series of potent 1,2,4-Oxadiazole EthR inhibitors. *Journal of Medicinal Chemistry* **55**, 68–83.

Flipo, M., Willand, N., Lecat-Guillet, N., Hounsou, C., Desroses, M., Leroux, F., Lens, Z., Villeret, V., Wohlkönig, A., Wintjens, R., Christophe, T., Kyoung Jeon, H., Locht, C., Brodin, P., Baulard, A. R. and Déprez, B. (2012*b*). Discovery of novel N-phenylphenoxyacetamide derivatives as EthR inhibitors and ethionamide boosters by combining high-throughput screening and synthesis. *Journal of Medicinal Chemistry* **55**, 6391–6402.

Frénois, F., Engohang-Ndong, J., Locht, C., Baulard, A. R. and Villeret, V. (2004). Structure of EthR in a ligand bound conformation reveals therapeutic perspectives against tuberculosis. *Molecular Cell* **16**, 301–307.

Hotta, K., Kitahara, T. and Okami, Y. (1975). Studies on the mode of action of amiclenomycin. *Journal of Antibiotics* **28**, 222–228.

Hudson, S. A., McLean, K. J., Munro, A. W. and Abell, C. (2012*a*). *Mycobacterium tuberculosis* cytochrome P450 enzymes: a cohort of novel TB drug targets. *Biochemical Society Transactions* **40**(3), 573–579.

Hudson, S. A., McLean, K. J., Surade, S., Yang, Y. Q., Leys, D., Ciulli, A., Munro, A. W. and Abell, A. (2012*b*). Application of fragment screening and merging to the discovery of inhibitors of the *Mycobacterium tuberculosis* cytochrome P450 CYP121. *Angewandte Chemie International Edition* **51**, 9311–9316.

Hudson, S. A., Surade, S., Coyne, A. G., McLean, K. J., Leys, D., Munro, A. W. and Abell, C. (2013). Overcoming the limitations of fragment merging: rescuing a strained merged fragment series targeting *Mycobacterium tuberculosis* CYP121. *ChemMedChem* **8**, 1451–1456.

Hung, A. W., Silvestre, H. L., Wen, S., Ciulli, A., Blundell, T. L. and Abell, C. (2009). Application of fragment growing and fragment linking to the discovery of inhibitors of *Mycobacterium tuberculosis* pantothenate synthetase. *Angewandte Chemie International Edition* **48**, 8452–8456.

Hung, A. W., Silvestre, H. L., Wen, S., George, G. P., Boland, J., Blundell, T. L., Ciulli, A. and Abell, C. (2016). Optimization of inhibitors of *Mycobacterium tuberculosis* pantothenate synthetase based on group efficiency analysis. *ChemMedChem* **11**, 38–42.

Jackson, M., Raynaud, C., Lanéelle, M. A., Guilhot, C., Laurent-Winter, C., Ensergueix, D., Gicquel, B. and Daffé, M. (1999). Inactivation of the antigen 85C gene profoundly affects the mycolate content and alters the permeability of the *Mycobacterium tuberculosis* cell envelope. *Molecular Microbiology* **31**, 1573–1587.

Kavanagh, M. E., Coyne, A. G., McLean, K. J., James, G. G., Levy, C. W., Marino, L. B., de Carvalho, L. P. S., Chan, D. S. H., Hudson, S. A.,

https://doi.org/10.1017/S0031182016001876 Published online by Cambridge University Press

Surade, S., Leys, D., Munro, A. W. and Abell, C. (2016). Fragment-based approaches to the development of *Mycobacterium tuberculosis* CYP121 inhibitors. *Journal of Medicinal Chemistry* **59**, 3272–3302.

Koul, A., Arnoult, E., Lounis, N., Guillemont, J. and Andries, K. (2011). The challenge for new drug discovery for tuberculosis. *Nature* **469**, 483–490.

Leys, D., Mowat, C. G., McLean, K. J., Richmond, A., Chapman, S. K., Walkinshaw, M. D. and Munro, A. W. (2003). Atomic structure of *Mycobacterium tuberculosis* CYP121 to 1·06 A reveals novel features of cytochrome P450. *Journal of Biological Chemistry* **278**, 5141–5147.

Mascarello, A., Mori, M., Chiaradia-Delatorre, L. D., Menegatti, A. C., Delle Monache, F., Ferrari, F., Yunes, R. A., Nunes, R. J., Terenzi, H., Botta, B. and Botta, M. (2013). Discovery of *Mycobacterium tuberculosis* protein tyrosine phosphatase B (PtpB) inhibitors from natural products. *PLoS ONE* **8**, e77081.

Mashalidis, E., Śledź, P., Lang, S. and Abell, C. (2013). A three-stage biophysical screening cascade for fragment-based drug discovery. *Nature Protocols* **8**, 2309–2324.

McLean, K. J., Carroll, P., Lewis, D. G., Dunford, A. J., Seward, H. E., Neeli, R., Cheesman, M. R., Marsollier, L., Douglas, P., Smith, W. E., Rosenkrands, I., Cole, S. T., Leys, D., Parish, T. and Munro, A. W. (2008). Characterization of active site structure in CYP121. A cytochrome P450 essential for viability of *Mycobacterium tuberculosis* H37Rv. *Journal of Biological Chemistry* **283**, 33406–33416.

Murray, C. W. and Blundell, T. L. (2010). Structural biology in fragment-based drug design. *Current Opinion in Structural Biology* **20**, 497–507.

Nikiforov, P. O., Surade, S., Blaszczyk, M., Delorme, V., Brodin, P., Baulard, A. R., Blundell, T. L. and Abell, C. (2016). A fragment merging approach towards the development of small molecule inhibitors of *Mycobacterium tuberculosis* EthR for use as ethionamide boosters. *Organic and Biomolecular Chemistry* **14**, 2318–2326.

Park, S. W., Klotzsche, M., Wilson, D. J., Boshoff, H. I., Eoh, H., Manjunatha, U., Blumenthal, A., Rhee, K., Barry, C. E., III, Aldrich, C. C., Ehrt, S. and Schnappinger, D. (2011). Evaluating the sensitivity of *Mycobacterium tuberculosis* to biotin deprtication using regulated gene expression. *PLoS Pathogens* **7**, e1002264, 1–0.

Rawls, K. A., Lang, T. P., Takeuchi, J., Imamura, S., Baguley, T. D., Grundner, C., Alber, T. and Ellman, J. A. (2009). Fragment-based discovery of selective inhibitors of the *Mycobacterium tuberculosis* protein tyrosine phosphatase PtpA. *Bioorganic and Medicinal Chemistry Letters* **19**, 6851–6854.

Sambandamurthy, V. K., Wang, X., Chen, B., Russell, R. G., Derrick, S., Collins, F. M., Morris, S. L. and Jacobs, W. R. (2002). A pantothenate auxotroph of *Mycobacterium tuberculosis* is highly attenuated and protects mice against tuberculosis. *Nature Medicine* **8**, 1171–1174.

Scheich, C., Puetter, V. and Schade, M. (2010). Novel small molecule inhibitors of MDR *Mycobacterium tuberculosis* by NMR fragment screening of antigen 85 °C. *Journal of Medicinal Chemistry* **53**, 8362–8367.

Schmidt, M. F., Groves, M. R. and Rademann, J. (2011). Dynamic substrate enhancement for the identification of specific, second-site-binding fragments targeting a set of protein tyrosine phosphatases. *ChemBioChem* **12**, 2640–2646.

Scott, D. E., Coyne, A. G., Hudson, S. A. and Abell, C. (2012). Fragment based approaches in drug discovery and chemical biology. *Biochemistry* **51**, 4990–5003.

Shi, C. and Aldrich, C. C. (2012). Design and synthesis of potential mechanism-based inhibitors of the aminotransferase BioA involved in biotin biosynthesis. *Journal of Organic Chemistry* **77**, 6051–6058.

Silvestre, H. L., Blundell, T. L., Abell, C. and Ciulli, A. (2013). Integrated biophysical approach to fragment screening and validation for fragment-based lead discovery. *Proceedings of the National Academy of Sciences of the United States of America* **110**, 12984–12989.

Singh, R., Rao, V., Shakila, H., Gupta, R., Khera, A., Dhar, N., Singh, A., Koul, A., Singh, Y., Naseema, M., Narayanan, P. R., Paramasivan, C. N., Ramanathan, V. D. and Tyagi, A. K. (2003). Disruption of mptpB impairs the ability of *Mycobacterium tuberculosis* to survive in guinea pigs. *Molecular Microbiology* **50**, 751–762.

Soellner, M. B., Rawls, K. A., Grundner, C., Alber, T. and Ellman, J. A. (2007). Fragment-based substrate activity screening method for the identification of potent inhibitors of the *Mycobacterium tuberculosis* phosphatase PtpB. *Journal of the American Chemical Society* **129**, 9613–9615.

Spry, C., Kirk, K. and Saliba, K. J. (2008). Coenzyme A biosynthesis: an antimicrobial drug target. *FEMS Microbiology Reviews* **32**, 56–106.

Surade, S., Ty, N., Hengrung, N., Lechartier, B., Cole, S. T., Abell, C. and Blundell, T. L. (2014). A structure-guided fragment-based approach for the discovery of allosteric inhibitors targeting the lipophilic binding site of transcription factor EthR. *Biochemical Journal* **458**, 387–394.

Tan, L. P., Wu, H., Yang, P. Y., Kalesh, K. A., Zhang, X., Hu, M., Srinivasan, R. and Yao, S. Q. (2009). High-throughput discovery of *Mycobacterium tuberculosis* protein tyrosine phosphatase B (MptpB) inhibitors using click chemistry. *Organic Letters* **11**, 5102–5105.

Tonks, N. K. (2006). Protein tyrosine phosphatases: from genes, to function, to disease. *Nature Reviews Molecular Cell Biology* **7**, 833–846.

Vannelli, T. A., Dykman, A. and Ortiz de Montellano, P. R. (2002). The antituberculosis drug ethionamide is activated by a flavoprotein monooxygenase. *Journal of Biological Chemistry* **77**, 12824–12829.

Villemagne, B., Flipo, M., Blondiaux, N., Crauste, C., Malaquin, S., Leroux, F., Piveteau, C., Villeret, V., Brodin, P., Villoutreix, B. O., Sperandio, O., Soror, S. H., Wohlkönig, A., Wintjens, R., Deprez, B., Baulard, A. R. and Willand, N. (2014). Ligand efficiency driven design of new inhibitors of *Mycobacterium tuberculosis* transcriptional repressor EthR using fragment growing, merging, and linking approaches. *Journal of Medicinal Chemistry* **57**, 4876–4888.

Wang, S. and Eisenberg, D. (2003). Crystal structures of a pantothenate synthetase from *M. tuberculosis* and its complexes with substrates and a reaction intermediate. *Protein Science* **12**, 1097–1108.

Webb, M. E., Smith, A. G. and Abell, C. (2002). Biosynthesis of pantothenate. *Natural Product Reports* **21**, 695–721.

Willand, N., Dirié, B., Carette, X., Bifani, P., Singhal, A., Desroses, M., Leroux, F., Willery, E., Mathys, V., Déprez-Poulain, R., Delcroix, G., Frénois, F., Aumercier, M., Locht, C., Villeret, V., Déprez, B. and Baulard, A. R. (2009). Synthetic EthR inhibitors boost antituberculous activity of ethionamide. *Nature Medicine* **15**, 537–544.

Woong Park, S., Klotzsche, M., Wilson, D. J., Boshoff, H. I., Eoh, H., Manjunatha, U., Blumenthal, A., Rhee, K., Barry, C. E., III, Aldrich, C. C., Ehrt, S. and Schnappinger, D. (2011). Evaluating the sensitivity of *Mycobacterium tuberculosis* to biotin deprivation using regulated gene expression. *PLoS Pathogens* **7**, e1002264.

World Health Organisation (2015). Global tuberculosis report, Geneva; (http://apps.who.int/iris/bitstream/10665/191102/1/9789241565059_eng.pdf?ua=1 (accessed October 2016).

https://doi.org/10.1017/S0031182016001876 Published online by Cambridge University Press